Time and frequency study of the induced potentials by the switching of the gradients during MRI

Karim Bouzrara[1], Odette Fokapu[2], Kais Jamoussi[3], Ahmed Fakhfakh[4]

[1]*University of Sousse, ENISo*

Digital Research Center of Sfax, LT2S, LR16CRNS01, Sfax, Tunisia
[1]karim.bouzrara17@gmail.com

[3]*Advanced Electronic Systems and Sustainable Energy Laboratory*

ENET'com, Sfax, Tunisia
[3]kais.jamoussi@yahoo.fr

Digital Research Center of Sfax, LT2S, LR16CRNS01, Sfax, Tunisia
ENET'com, Sfax, Tunisia
[4]ahmed.fakhfakh@enetcom.usf.tn

[2] *UMR 7338, GB, University of Technology of Compiegne, Royallieu, BP 20529,*

60205 Compiègne, France
[2]odette.fokapu@utc.fr

Abstract—**During Magnetic Resonance Imaging (MRI), the switching of the magnetic field gradients is useful to obtain images generated in parallel induced voltages. These strongly disturb the electrophysiological signals collected simultaneously. In an earlier article we presented a bench developed in the laboratory allowing in vitro collection of these "induced potentials" [1]. This work is devoted to specify of the temporal, statistical and frequency properties of these induced potentials. A stationary study is proposed according to two methods (KPSS and LMC) accompanied by an estimation of the spectral density according to the Welch method. The results show stationary in the weak sense. Significant changes in frequency characteristics appear depending on the imaging sequences and the orientation of the sections. This type of information is to be considered on the design of denoising algorithms in order to improve its robustness.**

Keywords—MRI, Potentials induced by the switching of gradients, stationary, power spectral density

I. INTRODUCTION

MRI techniques are constantly evolving, with the aim of improving the quality of images and widening the fields of application. The development of new strategies for a simultaneous observation by MRI and by electrophysiological signals of the organs explored. The works in the literature clearly indicate the scientific and clinical interest in combining information deduced from the MRI of the organ studied, and information extracted from the electrophysiological signal detected on the surface of this same organ.

These evolutions generate artifacts which "pollute" the electrophysiological signals collected simultaneously. These signals are useful for image synchronization monitoring and or patient monitoring. The artifacts are mainly due to the process of interaction between the electromagnetic devices responsible for obtaining MRI images and the electrophysiological acquisition devices used for monitoring and patient monitoring. [2-3]. The acquired electrophysiological signal can be modeled as the superposition of three sources of potentials :

$$S(t) = S_e(t) + S_{B0}(t) + S_{ind}(t) \text{ [3]}.$$

$S_e(t)$ represents the useful signal, $S_{B0}(t)$ the potential induced by the static magnetic field B0 and $S_{ind}(t)$ the voltages induced, by the commutations of the gradients; they have a high amplitude and located in the bandwidth of the signals $S_e(t)$. The solutions recommended in the literature are not completely satisfactory [4-5]. In addition, to limit disturbances, the amplifiers bandwidth used in MRI does not exceed 30 Hz, which is adequate to acquire ECG signals for image synchronization purposes [6]. Other types of investigations, such as combined EEG/EMG information with functional MRI (fMRI), require a larger bandwidth (40 Hz) to properly acquire the EEG/EMG signals [7]–[9]. Thus, the ECG signals are mainly used for monitoring subjects and synchronizing images. Providing ECG devices for diagnosis (frequency band> 30Hz) is topical in research [10]. New strategies are required. Deep knowledge of the signal contamination mechanism which contribute to develop an effective remediation solutions. The experimental device that we have developed and the process of processing the "noise sources" linked to the switching of the gradients allow this type of study.

II. MATERIAL AND METHOD

A. Acquisition of induced potentials

The bench having already been used to collect the induced potential is composed of different modules MRI-compatible as shown in Figure 1.
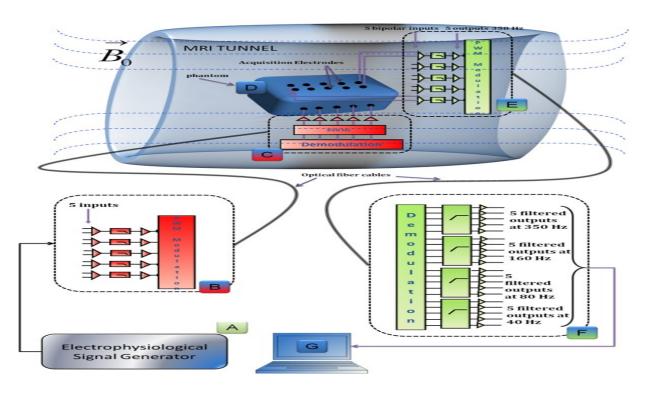
Fig. 1 Synoptic diagram of the experimental bench.

A detailed description was presented in a previous article [1]. This bench offers different types of experiments. This study allowed us through a model of conductive tissue placed in the tunnel and equipped with electrodes to collect the potentials induced after the MRI sequences activation. In this case, no signal is injected in the tunnel. the potentials induced after the MRI sequences activation. In this case, no signal is injected in the tunnel.

The induced potentials are taken at the bandwidth filter output (0.05-350Hz) and sampled at 10 kHz.

This bench includes two modules (B) and (C) for transmission, (E) and (F) for signal detection. An electrophysiological signal generator (A) is used to simulate the signal injected into the MRI tunnel via the transmitter (B), the optical fiber, and the non-magnetic receiver (C). The contaminated signals on the surface of the ghost (D) are detected by the non-magnetic transmitter (E) and are transmitted by a second optical fiber outside the faraday cage to the receiver (E). When the generator (A) is switched off, the system makes it possible to capture the potentials induced by the switching of the gradients. The detected signals are then acquired and processed at the processing station (G).

The measurements were performed on a GE Signa HDxt 1.5 Tesla clinical MRI. The parameters of the standard imaging sequences used are as follows:

FSE : 440/12/30/448x512 (TR/TE FOV/Mat)

CINE : 9.4/5.1/256 x 128/34 x 25 (TR/TE FOV/Mat)
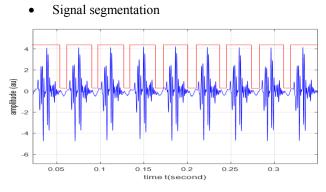
- Signal segmentation

Fig. 2 Potential induced coronal FSE sequences

A simple signal segmentation algorithm has been developed to extract epochs from the recorded signal (Fig. 2). These extracts correspond to the dominant part of the readout gradient artifacts.

The results of the segmentation are illustrated in Fig. 3, which indicates the temporal shape of the induced FSE potential in coronal section. In addition to a global analysis in time and frequency of the recordings, the successive puffs are characterized.
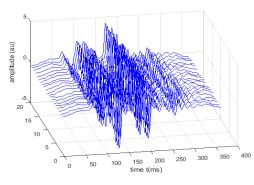
Fig. 3 Potentials induced by coronal FSE sequences

B. Identification of stationarity and spectral analysis

By definition, a process is said to be strictly stationary if and only if its statistical moments are independent over time.

An acquired time series will never have moments of any kind, a reason to consider a weaker definition of stationary.

1) The Kwiatkowski-Phillips-Schmidt-Shin stationary test: The KwiatkowskiPhillips-Schmidt-Shin (KPSS) test is widely used in econometrics for testing a null hypothesis in which a time series is weakly stationary against the alternative of a unit root [11]. This test is also used by Korürek and Özkaya to test for the stationarity of EEG [12]. In order to verify the Bresch et al. statement that the MR induced artifacts are stationary [13], the KPSS test was run on the recorded signal.
This KPSS test proposes that a signal can be estimated by a sum of a deterministic trend, a random walk and a stationary error according to (1)

$$y_t = \delta(t) + \xi_t + \varepsilon_t \qquad (1)$$

Where δ is the slope of the linear trend curve, ε_t is a stationary process and ξ_t is a random walk with equation (2):

$$\xi_t = \xi_{t-1} + v_t \quad \text{Ou} \quad v_t \approx i.i.d.(0, \sigma_v^2) \qquad (2)$$

2) Leybourne and McCabe stationarity test :
Leybourne and McCabe use a parametric version of the LM test of the null hypothesis of stationarity against the presence of a unit root. LMC test uses the structural model:

$$y(t) = c(t) + \delta t + b_1 y(t-1) + \cdots + b_p y(t-p) + u_1(t) \qquad (3)$$
$$c(t) = c(t-1) + u_2(t) \qquad (4)$$

When
$$u_1(t) \sim i.i.d.(0, \sigma_1^2)$$
$$u_2(t) \sim i.i.d.(0, \sigma_2^2)$$

and u_1 and u_2 are independent of each other.
The model is equivalent to the second order of the ARIMA model (p, 1,1) of reduced form.

$$(1-L)y(t) = \delta t + b_1(1-L)y(t-1) + \cdots + b_p(1-L)y(t-p) + (1-aL)v(t) \qquad (5)$$

Where L is the shift operator is

$$Ly(t) = y(t-l), et \ v(t) \sim i.i.d \ (0, \sigma^2) \qquad (6)$$

The null hypothesis is that $\sigma^2 = 0$ in the structural model, which is equivalent to a = 1 in the model in reduced form. The alternative is that $\sigma^2 = 0 > 0$ or a <1. Under null, the structural model is AR (p) with the interception c (0) and the trend δt; the reduced form model is a representation of the same over-differentiated ARIMA process (p, 1,1).
The statistical parameters of the stationary tests are illustrated in the following table.

TABLE 1
RESULTS OF THE STATIONNARITY TESTS

p-value	0.01	0.05	0.1
Level stationarity	0.739	0.463	0.347
Trend stationarity	0.216	0.146	0.119

This stationary study makes it possible to define the statistical parameters of the induced potentials. In order to validate these results, we used to know its spectral parameters. The power spectrum density is estimated by the Welch method. The spectrum parameters (fmean: the average frequency, fmed: the median frequency, fmax: the maximum frequency) of the global and local signal are calculated.
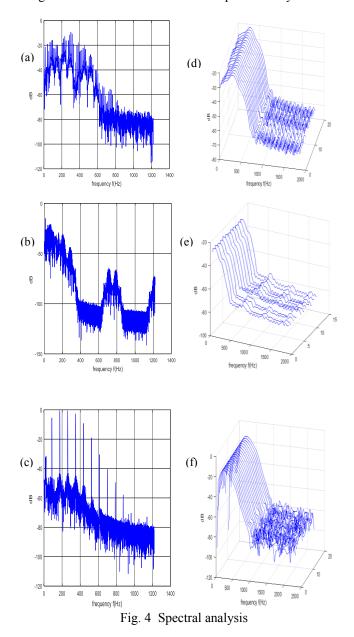In the next section, we will present the results of the stationary tests as well as the results of the spectral analysis.

III. RESULTS

The results of the stationary test are illustrated in Table 2.

TABLE 2
RESULTS OF THE STATIONNARITY TESTS

Sequence	KPSS	LMC	P_value
Ciné	0.0020	-0.0720	> 0.1
FSE	0.0678	-2.5338	> 0.1
SPGR03	0.1118	-15.3288	> 0.1
SPGR05	0.1034	-28.2931	> 0.1

The results of the tests presented in Table 2 confirm that the potential induced in an MRI environment is stationary in the weak sense, according to the following decision rule
-If η_u (or η_τ) is less than the critical value reported in table 1, then we accept the null hypothesis of stationarity.
-If η_u (or η_τ) is greater than the critical value reported in table 1, then we reject the null hypothesis of stationary.

Figures 4 illustrate the results of the spectral analysis.

Fig. 4 Spectral analysis

FIG. 4 is a spectral representation (a) of the coronal FSE sequences, (b) SPGR 05 and (c) cine Sagittal whose (d), (e) and (f) are the respective tridimensional segments representations (a), (b) and (c).

TABLE 3
SPECTRAL ANALYSIS RESULTS

F(Hz)	Average		Median		Maximum	
	Global	local	Global	Local	Global	Local
FSE coronal	248.2846	250.2769	273.4375	258.7891	300.2085	282.3203
Ciné sagittal	242.1070	233.8794	260.1460	245.3125	260.3667	245.3750
SPGR 03	91.3945	86.2871	106.6895	105.4688	15.0098	16.9036
SPGR 05	63.3566	65.1685	52.9785	54.6875	12.8926	10.8125

The tridimensional representation of the local spectrum indicate the same appearance for all the spectrum. The latter seem to have the same appearance as that of the global spectrum. These results are confirmed by the frequencies in Table 3.

TABLE 4
RELATIVE ERROR RATE

F(Hz)	Average	Median	Maximum
FSE coronal	1	5	5
Ciné sagittal	3	5	5
SPGR 03	5	1	6
SPGR 05	2	3	16

Table 4 illustrates the relative error rate between the global and the local frequency. The results indicate an average error rate of which the average which does not exceed 5%. Indeed, the average, median and maximum frequencies of the global spectrum are practically similar compared to that of the local spectrum, this proves that the processed signals are independent over time.

This is to be considered as an advantage in the development of a reliable denoising algorithm.

IV. DISCUSSION AND CONCLUSION

Throughout this article, we started with the segmentation of the induced potentials collected in an MRI environment, then we proceed with a stationary study and a spectral analysis. Spectral analysis of the artefact bursts taken from the same recording show almost constant frequency parameters, which confirms the stationary nature of the induced potentials indicated by the KPSS and LMC tests. On the other hand, when we consider the results from two cutting orientations in the same sequence, we observe significant variations, temporal and frequency characteristics. The results obtained lead us to validate the segmentation process, the stationary study and the spectral analysis on in vivo signals. This type of information is to be considered to develop a denoising algorithm for example in order to improve its robustness.

V. REFERENCES

[1]   O.Fokapu, A.El-Tatar, "An Experimental Setup to Characterize MR Switched Gradient-Induced Potentials," IEEE Transactions on Biomedical Circuits and Systems, vol. 7, no. 3, pp. 355-362, June 2013.

[2]   J. Felblinger and C. Boesch, "Patient monitoring in the MR environment", Interventional Magnetic Resonance Imaging, Springer-Verlag, pp.105–112, 1997.

[3]   J. Felblinger, J. Slotboom, R. Kreis, and B. Jung, "Restoration of electrophysiological signals distorted by inductive effects of magnetic field gradients during MR sequences", Magn. Reson. Med., vol. 41, no. 4, pp. 715-721, April 1999.

[4]   A. Guillou, J.M. Sellal, S. Ménétré, G. Petitmangin, J. Felblinger, L. Bonnemains, "Adaptive step size LMS improves ECG detection during MRI at 1.5 and 3 T MAGMA", Magnetic Resonance Materials in Physics, Biology and Medicine, vol. 30, pp. 567-577, December 2017.

[5]   M. Schmidt, J W. Krug and G. Rose, "Reducing of gradient induced artifacts on the ECG signal during MRI examinations using

Wilcoxon filter". Current Directions in Biomedical Engineering, vol. 2, no. 1, pp. 175-178, September 2016.

[6] J. Felblinger, C. Lehmann, and C. Boesch, "Electrocardiogram acquisition during MR examinations for patient monitoring and sequence triggering," Magn. Reson. Med., vol. 32, no. 4, pp. 523–529, Oct. 1994.

[7] R. I. Goldman, J. M. Stern, J. Engel, and M. S. Cohen, "Acquiring simultaneous EEG and functional MRI," Clin. Neurophys., vol. 111,no. 11, pp. 1974–1980, Nov. 2000.

[8] A.-F. van Rootselaar, N. M. Maurits, R. Renken, J. H. T. M. Koelman, J. M. Hoogduin, K. L. Leenders, and M. A. Tijssen, "Simultaneous EMG-functional MRI recordings can directly relate hyperkinetic movements to brain activity," Hum. Brain Mapp., vol. 29, no. 12, pp. 1430–1441, Dec. 2008.

[9] J. Z. Liu, T. H. Dai, T. H. Elster, V. Sahgal, R. W. Brown, and G. H. Yue, "Simultaneous measurement of human joint force, surface electromyograms, and functional MRI-measured brain activation," J. Neurosci. Meth., vol. 101, no. 1, pp. 49–57, Aug. 2000.

[10] J.E. Dos Reis, P. Soullié, J. Oster, E. Palmero Soler, G. Petitmangin, J. Felblinger, F. Odille, "Reconstruction of the 12‐lead ECG using a novel MR‐compatible ECG sensor network". Magn Reson Med, vol. 82, no. 5, pp. 1929-1945, June 2019.

[11] D. Kwiatkowski, P.C.B. Phillips, P. Schmidt, and Y. Shin, "Testing the null hypothesis of stationarity against the alternative of a unit root,"J. Econometrics, vol. 54, pp. 159–178, 1992.

[12] M. Korürek, and A. Özkaya, "A new method to estimate short-run and long-run interaction mechanisms in interictal state," Digit. Signal Process., vol. 20, pp. 347–358, 2010.

[13] E. Bresch, J. Nielsen, K. Nayak, and S. Narayanan, "Synchronized and noise-robust audio recordings during realtime magnetic resonance imaging scans," J. Acoust. Soc. Am., vol. 120, pp. 1791–1794, 2006.